Int. J. Multiphase Flow Vol. 13, No. 5, pp. 615–628, 1987
Printed in Great Britain.

0301-9322/87 $3.00 + 0.00

THE LIQUID FILM AND THE CORE REGION VELOCITY PROFILES IN ANNULAR TWO-PHASE FLOW

M. K. JENSEN

Department of Mechanical Engineering, Aeronautical Engineering and Mechanics, Rensselaer Polytechnic Institute, Troy, NY 12180-3590, U.S.A.

(*Received* 4 *October* 1985; *in revised form* 8 *April* 1987)

Abstract—Film flow data from complete data sets (i.e. those which have pressure gradient, film thickness and film flowrate) have been compared with three velocity profile correlations from the literature. The double velocity profile method was found to best represent the data. Velocity profile data in the core region of low-pressure air/water dispersed annular two-phase flow have been successfully correlated. A logarithmic law has been developed by making all calculations relative to the liquid film/gas core interface. The nondimensional velocity profile depends explicitly on the nondimensional distance from the interface, the entrainment and the nondimensional film thickness. The correlation correctly models the "laminarization" of the velocity profile with changing flow conditions. Qualitative comparisons are made with high-pressure steam/water two-phase flow velocity profile data.

INTRODUCTION

Because annular two-phase flow occurs so frequently in so many industrial situations, much time and effort has been expended in the development of mathematical models of this flow regime so that dependent variables such as film thickness, film flowrate and pressure gradient can be predicted. Various aspects of annular flow have been discussed in many publications (e.g. Hewitt & Hall-Taylor 1970; Wallis 1969). In this paper it will be assumed that the fluid flow in this regime can be broken into two parts: the film region and the core region. The liquid film on the tube walls has been addressed at some length in the literature and will only be discussed briefly here. Several different methods have been proposed for predicting the film flowrate from assumed velocity profiles; unfortunately, the number of complete data sets are scarce and these prediction methods have not been tested against a large number of data points. Hewitt & Hall-Taylor (1970) list and briefly discuss several different approaches to the problem. These methods either assumed a single velocity profile or a double velocity profile and may or may not take into account effects of curvature and variation of shear stress within the liquid film. In addition, different models for the eddy diffusivity were used. A planar liquid/gas interface was assumed. More recently, Dobran (1983a) has developed a prediction method which attempts to take into account the wavy character of the liquid film surface.

While the velocity profile in the liquid film on the tube walls has had much attention, little attention has been given to the velocity profile in the liquid/vapor core region of annular two-phase flows. The common procedure for handling the core region is to assume a homogeneous, uniform velocity mixture. This has been done in studies addressing pressure drop, entrainment, turbulent viscosity, heat transfer, film thickness and film flow (e.g. Anderson & Mantzouranis 1960; Dobran 1983a, b; Hewitt & Hall-Taylor 1970; Levy 1966; Van der Welle 1981; Wallis 1969). However, as has been shown, for example, by Gill *et al.* (1964) and Adorni *et al.* (1960), the core region velocity profile can have a variety of shapes. For some combinations of conditions, the two-phase velocity profile can be relatively blunt, resembling a single-phase turbulent velocity profile; for other conditions, the two-phase velocity profile can resemble a single-phase laminar velocity profile. Thus, to assume a uniform velocity profile could cause significant errors. Few investigations have been performed to measure the two-phase velocity profile. Gill *et al.* (1963a, b, 1964) and Adorni *et al.* (1960) measured the velocity profiles in the core regions of annular flows where entrainment was large in some cases. Kuznetsov & Darmono (1978) measured velocity profiles in the core region of flows where entrainment is assumed to have been very low; how the liquid was introduced into

the test section is not discussed nor is an estimate of entrainment given. Velocity profiles in lower quality flows (in the bubbly-slug flow regimes) have been examined, for example, by Burdukov *et al.* (1979), Bankoff (1960) and Theofanous & Sullivan (1982).

The only studies found which give an expression for the two-phase velocity profile in the core region are by Turner (1966), Kashcheev & Muranov (1976) and Abolfadl & Wallis (1985). Turner (1966) assumes a 1/7 power law velocity profile in the core but gives no comparisons with actual data. Kashcheev & Muranov (1976) present a theoretically obtained expression which compares well with some high-pressure (69 b) steam/water data obtained from another investigation. (Unfortunately, not enough information is given about this experimental data to quantitatively compare it with the expression developed in the present study.) However, to use this complex expression quantities such as "angular frequency of the [turbulent] velocity pulsations of the carrier flow" must be estimated. Abolfadl & Wallis (1985) present an analysis using an experimentally determined mixing length in a differential analyses of annular two-phase flow. Used in conjunction with the shear stress profile, an integral equation was developed for the velocity profile in the core region.

There were two objectives in this study. First, several representative film flow models were to be tested against a large and diverse body of complete data. If indicated, an improved correlation would be developed. Second, because of the lack of a simple expression for the two-phase velocity profile in the core region of an annular flow, a predictive equation would be developed. The objective was to develop an empirical correlation using common quantities which would accurately model the different two-phase velocity profiles observed in experimental studies.

ANALYSIS AND DISCUSSION OF FILM FLOWRATE

A triangular interrelationship exists between the three dependent variables: film thickness, film flowrate and pressure gradient. Knowing any two of these permits evaluation of the third. To evaluate the film flowrate, W_f^+, the following integral, [1], which takes into account curvature effects, can be evaluated if the nondimensional film velocity profile $u_f^+ = u_f/u_f^*$ is known:

$$W_f^+ = \int_0^{\delta_f^+} u_f^+ \left(1 - \frac{y_f^+}{\mathrm{Re}_f^*}\right) \mathrm{d}y_f^+ \qquad [1]$$

In this expression $\delta_f^+ = \delta u_f^* \rho_f/\mu_f$, $\mathrm{Re}_f^* = R_0 u_f^* \rho_f/\mu_v$ and $y_f^+ = y u_f^* \rho_f/\mu_f$, where the subscript f refers to film properties, the superscript + refers to nondimensional quantities, R_0 is the tube radius, δ is the film thickness, u is the velocity, ρ is the density, μ is the dynamic viscosity, Re is the Reynolds Number, y is the distance from the wall and $u_f^* = \sqrt{\tau_w/\rho_f}$ is the friction velocity using the wall shear stress τ_w.

Three representative models of the velocity profile were investigated: a single velocity profile using the universal velocity profile; a double velocity profile using the universal velocity profile up to $y_f^+ = \delta_f^+/2$ and using an inverted reflection of the universal velocity profile for $\delta_f^+/2 < y_f^+ \leqslant \delta_f^+$; and the velocity profile developed by Dobran (1983a), which takes into account a wavy layer in the liquid film.

For the single velocity profile, the universal velocity profile was integrated using [1]. The following expressions for the total film flowrate were obtained:

$$\begin{aligned}
\delta_f^+ \leqslant 5, \quad & W_f^+ = \frac{(\delta_f^+)^2}{2} - \frac{(\delta_f^+)^3}{3}\mathrm{Re}_f^*, \\
5 < \delta_f^+ \leqslant 30, \quad & W_f^+ = 12.51 - 8.05\delta_f^+ + 5\delta_f^+ \ln(\delta_f^+) \\
& \quad + \frac{1}{\mathrm{Re}_f^*}[65.8 + 2.78\delta_f^+ - 2.5(\delta_f^+)^2 \ln(\delta_f^+)], \qquad [2] \\
\delta_f^+ > 30, \quad & W_f^+ = -63.9 + 3\delta_f^+ + 2.5\delta_f^+ \ln(\delta_f^+) \\
& \quad + \frac{1}{\mathrm{Re}_f^*}[649.5 - 2.125(\delta_f^+)^2 - 1.25(\delta_f^+)^2 \ln(\delta_f^+)].
\end{aligned}$$

Integrating the double velocity profile results in the following expressions:

$$\delta_f^+ \leqslant 10, \quad W_f^+ = \frac{(\delta_f^+)^2}{2} - \frac{(\delta_f^+)^3}{3}\mathrm{Re}_f^*,$$

$$10 < \delta_f^+ \leqslant 60, \quad W_f^+ = -3.05\delta_f^+ + 5\delta_f^+ \ln\left(\frac{\delta_f^+}{2}\right) + 1/\mathrm{Re}_f^* [17.22 + 22.26\delta_f^+ + 0.594(\delta_f^+)^2 - 2.5(\delta_f^-)^2 \ln\left(\frac{\delta_f^+}{2}\right), \quad [3]$$

$$\delta_f^+ > 60, \quad W_f^+ = 5.5\delta_f^+ + 2.5\delta_f^+ \ln\left(\frac{\delta_f^+}{2}\right) + \frac{1}{\mathrm{Re}_f^*}\left[1146 - 63.9\delta_f^+ - 3.688(\delta_f^+)^2 - 1.25(\delta_f^+)^2 \ln\left(\frac{\delta_f^+}{2}\right)\right].$$

The Dobran (1983a) expression, which takes into account the wavy interface, is as follows:

$$W_f^+ = W_f^+(\delta_t^+) + (\delta_f^+ - \delta_t^+) \times \left\{u^+(\delta_t^+) + \frac{(\delta_f^+ - \delta_t^+)}{2\left(\frac{\mu_{\mathrm{eff}}}{\mu_L}\right)}\left[1 - \left(1 - \frac{\tau_i}{\tau_w}\right)\frac{\delta_f^+ + 2\delta_t^+}{3\delta_f^+}\right]\right\}, \quad [4]$$

where $W_f^+(\delta_t^+)$ is obtained from the integrated single velocity profile assuming $\mathrm{Re}_f^* \to \infty$. The viscosity expression is given by $(\mu_{\mathrm{eff}}/\mu_L) = 1 + 0.0016(\delta_f^+ - \delta_t^+)^{1.8}$. The continuous nonwavy layer thickness δ_t^+ is given by

$$\frac{\delta_t^+}{D^+} = 140\, N_L^{0.433}\, \mathrm{Re}_c^{-1.35},$$

where

$$D^+ = \rho_L \frac{Du^*}{\mu_L},$$

$$N_L = \left[gD^3 \frac{\rho_L(\rho_L - \rho_G)}{\mu_L^2}\right]^{1/2},$$

$$\mathrm{Re}_c = u_c \rho_c \frac{D}{\mu_G},$$

u_c = the superficial gas velocity

and

ρ_c = the homogeneous density of the core.

The expression for the velocity at the edge of the nonwavy layer $u^+(\delta_t^+)$ is given by

$$\delta_t^+ \leqslant 5, \quad u^+ = \delta_t^+,$$

$$5 < \delta_t^+ \leqslant 30, \quad u^+ = -3.05 + 5 \ln(\delta_t^+),$$

$$\delta_t^+ > 30, \quad u^+ = 5.5 + 2.5 \ln(\delta_t^+). \quad [5]$$

These three models were used to predict the data from seven investigations which measured the three dependent quantities. Two quantities (film thickness and flowrate) can be used directly, but the third—pressure gradient—must be broken down into its component parts (friction, acceleration and hydrostatic) so that the wall shear stress can be evaluated.

The wall shear stress τ_w can be evaluated from a momentum balance on the liquid film:

$$\tau_w = \tau_i\left(\frac{R_i}{R_0}\right) - \frac{1}{2}\left(\pm\rho_f g - \frac{\partial P}{\partial z}\right)\left(\frac{R_0^2 - R_i^2}{R_o}\right), \quad [6]$$

where τ_i is the interfacial shear stress, R_i is the radius at the liquid film interface, g is gravity and

$\partial P/\partial z$ is the nonaccelerational pressure gradient. In the symbol ($\pm$), + represents upflow and − represents down flow. The interfacial shear can be found from

$$\tau_i = -\frac{R_i}{2}\left(\pm \rho_c g + \frac{\partial P}{\partial z}\right). \quad [7]$$

Assuming a homogeneous core (which will be discussed in the next section), the core density ρ_c can be obtained from

$$\rho_c = \epsilon_c \rho_G + (1 - \epsilon_c)\rho_L, \quad [8]$$

where the core void fraction ϵ_c is from

$$\epsilon_c = \frac{1}{1 + \left(\frac{\rho_G}{\rho_L}\right)(1-x)\frac{E}{x}}. \quad [9]$$

The subscript c represents core quantities, x is the quality and E is the entrainment in the core and is equal to the entrained liquid mass flow divided by the total liquid flow. The hydrostatic component of the pressure gradient is small so that the particular method of evaluation of ρ_c is not critical.

The nonacceleration pressure gradient is calculated by subtracting the acceleration pressure gradient from the total pressure gradient. The acceleration pressure gradient can be found by applying the momentum equation to the flow. By taking into account the nonuniform velocity profile in the core region by using a momentum flux factor β (which relates the nonuniform velocity profile momentum to an equivalent uniform velocity flow) the following equation is obtained:

$$\left(\frac{dP}{dL}\right)_{accel} = \beta\left(\frac{m_G}{A\rho_G}\right)^2 \frac{d\rho_G}{dL} + \beta\frac{m_L m_G}{A^2\rho_G^2}\left(E\frac{d\rho_G}{dL} + \rho_G\frac{dE}{dL}\right). \quad [10(a)]$$

The density gradient $d\rho/dL$ can be evaluated using the perfect gas law (all the data to be analyzed were obtained in air/water systems) and the total pressure gradient. Approximating the core velocities from Gill *et al.* (1963b) with a power law relationship, the exponent in the power law varies from about 1/7 to 1/3 which results in β varying from 1.02 to 1.09. Therefore, an average value of 1.055 was used. The quantity A is the cross-sectional area of the tube, m_G is the gas mass flow and m_L is the liquid mass flow. The entrainment gradient dE/dL was found by a method proposed by Kataoka & Ishii (1983). This correlation, for the case where $E/E_\infty \leqslant 1$, is as follows:

$$\frac{dE}{d\left(\frac{z}{D}\right)} = 2.87 \times 10^{-9}\,\mathrm{Re}_f^{0.5}\,\mathrm{Re}_{ff\infty}^{0.25}\,\mathrm{We}\left(1 - \frac{E}{E_\infty}\right)^2 + 2.64 \times 10^{-6}\,\mathrm{Re}_f^{-0.075}\,\mathrm{We}^{0.925}\left(\frac{\mu_G}{\mu_L}\right)^{0.26} + (1-E)^{0.185} - 0.088\,\mathrm{Re}_f^{-0.26}\left(\frac{\mu_G}{\mu_L}\right)^{0.026} E^{0.74}. \quad [10(b)]$$

The equilibrium entrainment E_∞ is given by

$$E_\infty = \tanh(7.25 \times 10^{-7}\,\mathrm{We}^{1.25}\,\mathrm{Re}_f^{0.25}), \quad [10(c)]$$

where Re_f is the total liquid Reynolds number, $\mathrm{Re}_f = \rho_L j_L D/\mu_L$, $\mathrm{Re}_{ff\infty} = \mathrm{Re}_f(1 - E_\infty)$ and $\mathrm{We} = \rho_G j_G^2 D[(\rho_L - \rho_G)/\rho_G]^{1/3}/\sigma$. The quantities j_L and j_G are the superficial liquid and gas velocities, respectively, σ is the liquid surface tension and z is the axial position.

Seven studies (all low-pressure air/water systems) were found which gave all three required pieces of data. Both upflow (Gill *et al.* 1963a, b) 1964; Ueda & Nose 1974; Whalley *et al.*, 1974) and downflow (Andreussi & Zanelli 1979; Chien & Ibele 1964; Ueda & Tanaka 1974) conditions were examined. Wide ranges of flows, qualities and entrainment levels were covered. Operating conditions ranged from strongly developing (Gill *et al.* 1963a, b) to quasi-equilibrium flow. Four of the papers had tabulated data while the other three gave graphical data.

Table 1. Comparison of film flowrate prediction methods with data from each investigation

	$\delta_f^+ \leqslant 25$			$\delta_c^+ > 25$			Total		
Reference	N	R	D	N	R	D	N	R	D
Andreussi & Zanelli (1979)	11			45			56		
1		0.762	0.238		0.842	0.158		0.827	0.173
2		0.854	0.155		0.946	0.068		0.928	0.085
3		0.835	0.176		0.794	0.208		0.802	0.202
4		1.118	0.236		1.021	0.072		1.040	0.104
Chien & Ibele (1964)	0			15			15		
1					0.830	0.174		0.830	0.174
2					0.910	0.114		0.910	0.114
3					0.733	0.268		0.733	0.268
4					0.851	0.158		0.851	0.158
Gill *et al.* (1963a, b)	0			48			48		
1					1.000	0.070		1.000	0.070
2					1.140	0.140		1.140	0.140
3					0.935	0.079		0.935	0.079
4					1.068	0.079		1.068	0.079
Gill *et al.* (1964)	20			15			35		
1		0.985	0.152		0.923	0.087		0.958	0.124
2		1.086	0.172		1.014	0.084		1.068	0.134
3		1.204	0.253		1.010	0.056		1.121	0.168
4		1.142	0.221		1.071	0.077		1.111	0.159
Ueda & Nose (1974)	0			21			21		
1					0.723	0.277		0.723	0.277
2					0.795	0.205		0.795	0.205
3					1.504	0.504		1.504	0.504
4					0.881	0.119		0.881	0.119
Ueda & Tanaka (1974)	0			13			13		
1					0.946	0.082		0.946	0.082
2					1.027	0.044		1.027	0.044
3					0.902	0.098		0.902	0.098
4					1.033	0.042		1.033	0.042
Whalley *et al.* (1974)	76			57			133		
1		0.941	0.210		0.845	0.155		0.890	0.186
2		1.053	0.220		0.953	0.092		1.010	0.165
3		1.040	0.195		0.876	0.153		0.970	0.177
4		0.959	0.140		0.983	0.103		0.969	0.124
Total	107			214			321		
1		0.931	0.202		0.878	0.141		0.895	0.161
2		1.039	0.204		0.985	0.107		1.003	0.139
3		1.050	0.204		0.934	0.181		0.973	0.188
4		1.009	0.165		1.000	0.081		1.003	0.116

1—Single velocity profile; 2—Double velocity profile; 3—Dobran; 4—Modified double velocity profile.

Table 1 shows how well the three correlations predict the data. (The division at $\delta_f^+ = 25$ resulted from examination of the plotted data.) The symbol N represents the number of data points; R represents the average ratio of the predicted film flowrate to the experimental flowrate; D represents the average ratio of the absolute deviation between the predicted film flowrate and the experimental flowrate to the experimental flowrate. Overall, the double velocity profile method predicted the data best. It went more closely through the center of the data and had the smallest average deviation. Figure 1 shows the ratio of the predicted flow using the double velocity profile to the experimental flow as a function of δ_f^+. As can be seen there is considerably more scatter at the smaller film thickness. This is probably a result of experimental inaccuracies; the film thicknesses represented by $\delta_f^+ \leqslant \sim 25$ are in the range of 0.1 mm and smaller. This small distance is difficult to measure. Note that regardless of the flow direction or whether it was strongly developing or quasi-equilibrium the data were predicted equally well.

To improve the predictions the data were plotted against a variety of quantities (e.g. figure 1) to determine if a pattern would emerge. However, other than that shown in figure 1, no other figures indicated any strong dependence on another quantity, although Re_f^* showed a weak dependence. Hence, using a nonlinear regression analysis, the following equations were developed by which the prediction from the double velocity profile method could be improved:

$$W_f^+ = CW^+_{f,\text{ double velocity profile}},$$

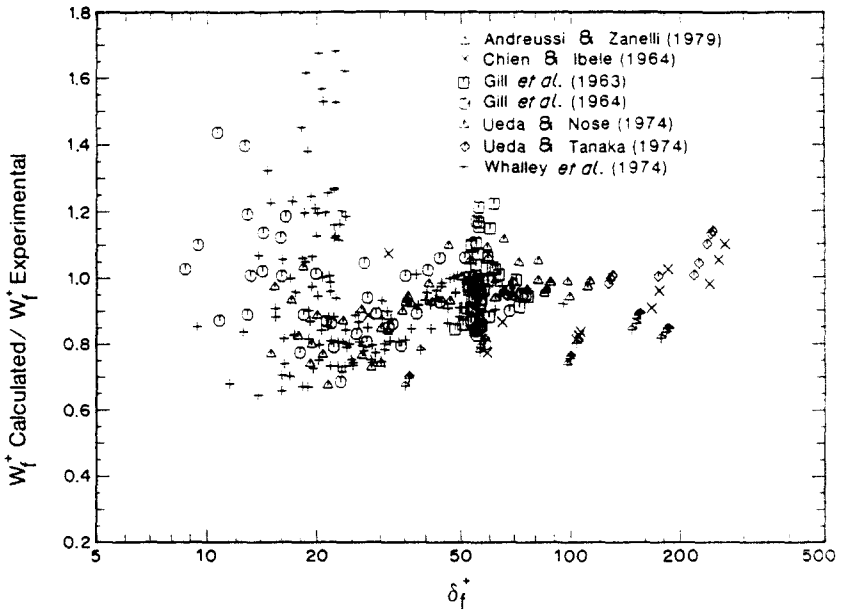

Figure 1. Deviations between film flowrate calculated with the double velocity profile and experimental data.

where

$$\delta_f^+ \leqslant 25, \quad C = 43.7(\delta_f^+)^{0.641}(\mathrm{Re}_f^*)^{-0.740},$$

$$\delta_f^+ > 25, \quad C = 5.13(\delta_f^+)^{-0.044}(\mathrm{Re}_f^*)^{-0.184}. \qquad [11]$$

The predictions using these equations also are shown in table 1 and figure 2. The overall predictions are improved but only by a small amount; the predictions for $\delta_f^+ \leqslant 25$ are improved more than those for $\delta_f^+ > 25$. Because of the marginal improvement using [11] compared to the unmodified double velocity profile, and because the results of the Dobran prediction method are not significantly different either, it is recommended that the double velocity profile be used.

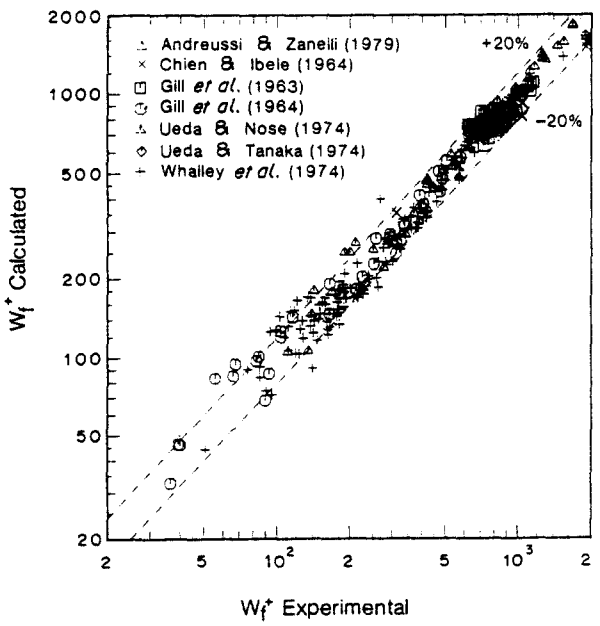

Figure 2. Comparison between predicted W_f^+ using the modified double velocity profile and experimental W_f^+.

ANALYSIS AND DISCUSSION OF CORE VELOCITY PROFILE

Gill *et al.* (1964) measured core velocity profiles over a wide range of fluid conditions. At a given air flow, as the water flow increased the peak (or centerline) velocity increased and the velocity near the wall decreased. Thus, at low qualities the velocity profile was blunt and was not much different than single-phase turbulent flow velocity profiles; at higher qualities the velocity profile was much more peaked, similar to a velocity profile characterized by single-phase laminar flow. They obtained this data from an experiment using a vertically upward air/water flow at near atmosphere pressure. The tube was 3.18 cm in diameter and pitot tube traverses were made 531 cm from the entrance of the pipe. The pitot tube was used to measure the mixture impact pressure and liquid flowrate at a point. Also measured were the liquid film thickness and pressure gradient at the sampling location. Because of the complete set of measurements, this data was chosen to be analyzed in detail. It is tabulated in Gill *et al.* (1963a, b). Note that this was not an equilibrium flow condition.

The local linear mixture velocity was calculated by assuming that the two-phase mixture behaved as a homogeneous single-phase fluid (Gill *et al.* 1963a, b), where the impact pressure ΔP_i is expressed as

$$\Delta P_i = \tfrac{1}{2}\rho_m u_m^2, \qquad [12]$$

ρ_m and u_m are the mixture mean density and mixture linear velocity, respectively. Using [13] to evaluate ρ_m, [12] can be rewritten in terms of the superficial liquid (G_G) and gas (G_L) mass velocities:

$$\rho_m = \frac{\rho_G \rho_L (G_G + G_L)}{(G_G \rho_L + G_L \rho_G)}. \qquad [13]$$

The superficial liquid mass velocity and impact pressure were both measured. Therefore, the superficial gas mass velocity and the local linear mixture velocities could be calculated.

To validate the homogeneous fluid assumption it is necessary to show that the slip ratio of the droplets in the core is near unity. A length mean drop diameter of each of the flows was calculated using the expression developed by Tatterson *et al.* (1977). Using this diameter and assuming the drop Reynolds number (using the relative velocity between the drop and the gas) is in the order of unity then, from Stoke's flow, an expression for the slip ratio can be obtained. Slip ratios from about 1 to 1.03 were obtained for all cases which resulted in the drop Reynolds numbers ranging downward from slightly above unity. Thus, the homogeneous fluid assumption for the core region is reasonable for the range of data examined.

Gill *et al.* (1964) demonstrated that the two-phase velocity profiles for given flow conditions plotted as straight lines on a graph of u_m as a function of the logarithm of (y/R_0). The straight line relationship is the same as that which occurs in single-phase turbulent flow. However, the slope of an individual two-phase velocity curve changes with changing flow conditions. For single-phase turbulent flows the slope is a constant regardless of flow conditions; with rough walls (which would be somewhat analogous to wavy film flow in annular flow) the slope is essentially the same as for smooth walls although the intercept is shifted downward with increasing roughness. Thus, the two-phase velocity profile in annular flow has some strong similarities and dissimilarities with single-phase turbulent flow. Therefore, single-phase flow expressions for the velocity profile were used as guidance in developing a two-phase flow velocity profile.

For fully rough turbulent single-phase flow the velocity profile [14] can be expressed in terms of three nondimensional groups. The expression (Kays & Crawford 1980)

$$u^+ = \frac{1}{k} \ln\left(\frac{32.6\, y^+}{\mathrm{Re}_r} + 1\right) \qquad [14]$$

relates the nondimensional velocity u^+ to the distance from the wall y^+ and to a roughness Reynolds number $\mathrm{Re}_r = tu^*\rho/\mu$. In this expression t is the height of the wall roughness elements. For two-phase flows it seems reasonable to assume that analogous quantities will be involved in the two-phase velocity profile; in addition, several other quantities applicable to two-phase annular flow could influence the process. By analogy to the roughness Reynolds number used in single-phase turbulent flow in tubes with rough walls, an expression to take into account the

roughness of the interface of the liquid film on the wall had to be developed. Gill *et al.* (1964) have shown that the effective roughness height of the liquid film is proportional to the film thickness. Thus, it seemed appropriate to describe an interface roughness parameter δ_c^+ in terms of the film thickness, interfacial shear and core properties:

$$\delta_c^+ = \delta \frac{u_c^* \rho_c}{\mu_c}. \quad [15]$$

The other parameter which was assumed to explicitly influence the two-phase velocity profile was the total amount of entrained liquid in the core, $(1-x)E$. With increasing liquid droplets in the core, turbulence would be suppressed. This would affect the development of the velocity profile. Hence, the following expression was chosen to serve as the basis for a correlation for predicting the core region two-phase velocity profile:

$$u_c^+ = f(y_c^+,\ \delta_c^+,\ (1-x)E). \quad [16]$$

It was felt that these quantities, if expressed in a manner appropriate to a two-phase annular flow, were those most likely to lead to the successful formulation of a predictive equation. The functional relationship would be found from the experimental data.

In single-phase flow, the nondimensional quantities are all defined relative to the wall conditions. For the core region of annular two-phase flow the quantities should be defined relative to the interface condition. Thus, the core nondimensional velocity would be defined by

$$u_c^+ = \frac{(u - u_i)}{u_c^*}, \quad [17]$$

where u_i is the interface velocity and $u_c^* = \sqrt{\tau_i/\rho_c}$ is the core friction velocity.

To determine the interface velocity, the liquid film velocity must be determined. The double velocity profile method developed by Anderson & Mantzouranis (1960) was used. The equations used for the double velocity profile interface velocity are

$$\begin{aligned} &\delta_f^+ \leqslant 10, \quad u_f^+ = \delta_f^+, \\ &10 < \delta_f^+ \leqslant 60, \quad u_f^+ = -6.10 + 10 \ln\left(\frac{\delta_f^+}{2}\right), \\ &\delta_f^+ > 60, \quad u_f^+ = 11.0 + 5.0 \ln\left(\frac{\delta_f^+}{2}\right). \end{aligned} \quad [18]$$

It should be noted that the interface velocity calculated using this assumed profile can be significant relative to the core mixture velocity. The ratio of interface velocity to peak core velocity ranged from about 0.001 to 0.10; the ratio of interface to average core velocity would be greater.

The nondimensional distance from the film/core interface was defined by

$$y_c^+ = \frac{(y - \delta) u_c^* \rho_c}{\mu_c}. \quad [19]$$

The core dynamic viscosity μ_c was calculated with an equation developed by Ishii & Zuber (1979):

$$\mu_c = \mu_G \epsilon_c \frac{-2.5(\mu_L + 0.4\mu_G)}{(\mu_L + \mu_G)}. \quad [20]$$

The data tabulated by Gill *et al.* (1964) were used to determine the functional relationship described by [16]. This data included local impact pressures, liquid superficial mass velocities, total entrained liquid flowrate, liquid film thickness, quality and nonacceleration pressure gradient. Only those tests where all the data were given were used. Gill *et al.* (1964) mentioned difficulties in measuring core velocities near the wall and stated that large errors could be present in the data from near the wall. Therefore, only data for $r/R < 0.8$ were used which resulted in 451 local

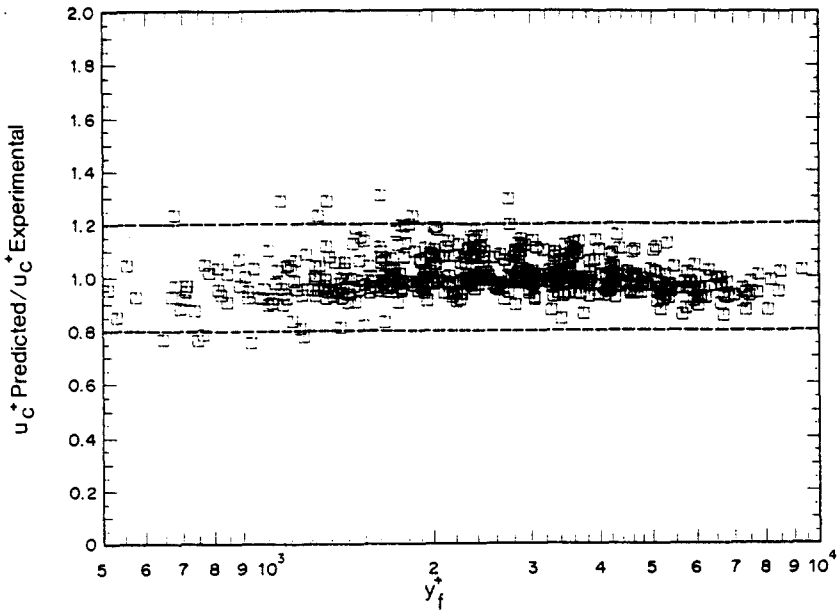

Figure 3. Deviations between predicted u_c^+ and experimental u_c^+. Data from Gill *et al.* (1964).

velocity data points from 41 test runs being analyzed initially. The ranges of the experimental conditions covered by this data were

$$37 < G < 250 \text{ kg/m}^2\text{ s},$$
$$0.14 < x < 0.94,$$
$$0.008 < E < 0.57,$$
$$19.9 < \delta_c^+ < 262,$$
$$460 < y_c^+ < 9300$$

and

$$0.0006 < (1-x)E < 0.38.$$

A nonlinear regression analysis was used to obtain a correlating equation for the velocity profile. Several expressions were tested, and the best one obtained was simple and relatively accurate. To improve the correlation, Chauvenet's criterion (Schenck 1979), which is a statistical procedure, was used to reject outlying points. A total of 9 points were rejected. The remaining points were used in the nonlinear regression analysis to determine the final correlating equation,

$$u_c^+ = \{4.22 + 14.05[(1-x)E]^{2.96}\} \ln(y_c^+) + 0.963 - 4.43 \ln(\delta_c^+) \quad [21]$$

which fitted the data well. Figure 3 is a scatter plot showing the deviations between the experimental data and the predictions from [21]. There appears to be a random scatter in the predictions. The average ratio of predicted to experimental velocity was 1.00; the mean absolute deviation between the predictions and the data was 0.062; the r.m.s. deviation was 0.083. [The present velocity profile correlation was compared to the expression developed by Abolfadl & Wallis (1985). While the predicted velocity profiles for every test run in Gill *et al.* (1964) were not compared, those which were showed excellent agreement.]

Figures 4 and 5 give typical velocity profile plots. The prediction equation correctly models the behavior of the flows. The changing shape of the velocity profiles, such as shown in figure 5, is predicted well. Figures 4 and 5 also illustrate one of the shortcomings of this correlation. The

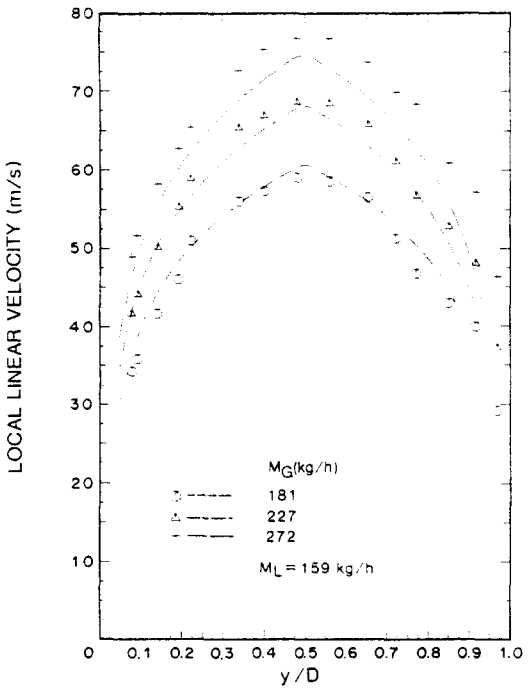

Figure 4. Comparison between typical experimental velocity profiles and predicted profiles. Data from Gill *et al.* (1964).

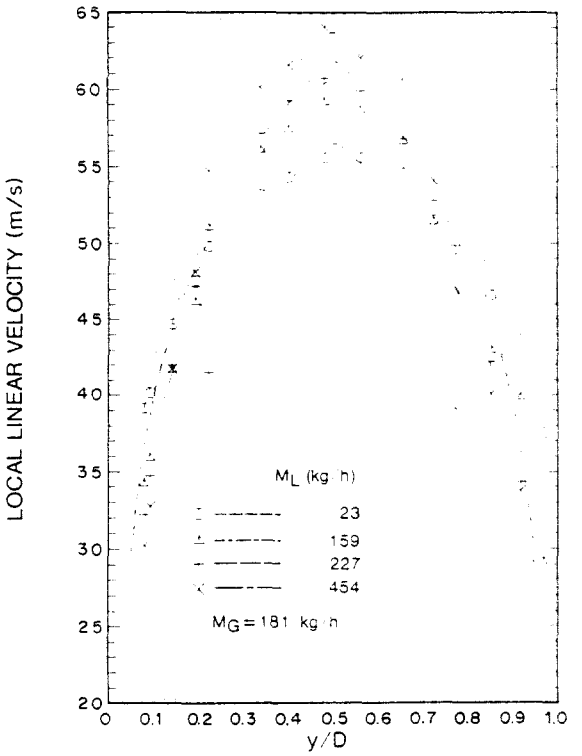

Figure 5. Comparison between typical experimental velocity profiles and predicted profiles. Data from Gill *et al.* (1964).

velocity gradient does not go to zero at the tube centerline. In addition, the velocity gradient goes to infinity at the interface. However, this correlation is intended to model the velocity over the majority of the core and was fitted accordingly. A separate correlation must be developed for the core velocity from the film/core interface to some distance into the core. Several assumed profiles (a quadratic and a cubic equation) were developed to match velocities and shear stresses at the film/core interface and at a short distance (based on effective film roughness) into the core. These equations did not predict monotonically increasing velocities from the interface to the point at which these velocities had to match the velocity predicted with [21]. In fact, the velocity profiles peaked between these two points. Thus, more work is required to handle the velocities close to the film/core interface.

One test of the usefulness of [21] for various flows is to integrate the velocity profile over the core area and compare the calculated core flows with the experimental values. This was done (acknowledging that the velocity near the film/core interface is imperfectly modeled) using the 321 complete data sets from the first part of this paper. The average ratio of predicted core flow to experimental core flow was 1.050 and the average absolute deviation between the predicted and experimental core flows was 0.119. [It should be noted that five points from Whalley *et al.* (1974) were overpredicted by more than 90%; eliminating these five points reduces the average ratio and average absolute deviation to 1.033 and 0.102, respectively.] This good agreement is encouraging as to the usefulness of [21].

The two-phase velocity profiles vary from being relatively blunt to being very peaked. The increasing "laminarization" of the velocity profile coincides with increasing total entrained liquid fraction $(1-x)E$. Typical profiles for different levels of total entrained liquid fraction are shown in figure 6 for various flowrates and qualities. At very low values of $(1-x)E$ the velocity profile is very close to that which would be obtained for a single-phase turbulent flow in a channel with rough walls. As $(1-x)E$ increases the velocity profile takes on a more parabolic shape typical of a laminar single-phase flow. Note, though, the velocity profile is affected by both $(1-x)E$ and δ_f^+. This is more clearly seen in figure 7. Several single-phase and two-phase velocity profiles are compared. The following single-phase flow equations (Kays & Crawford 1980) were used in

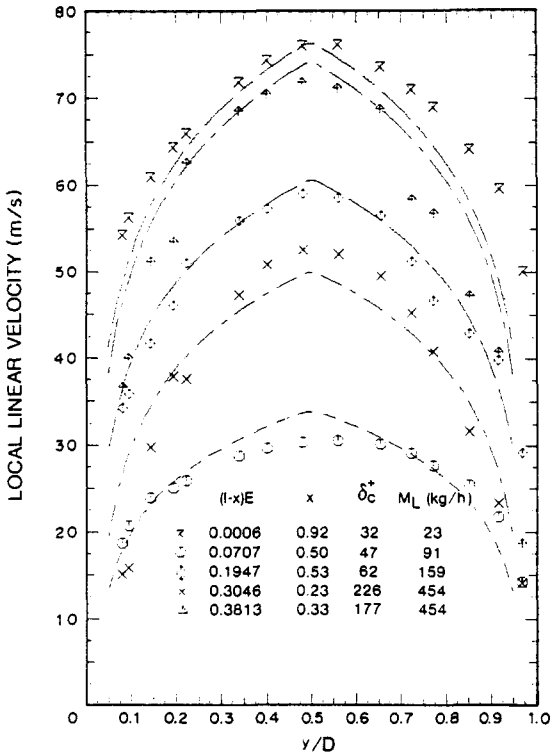

Figure 6. Variation in velocity profile with increasing total entrained liquid fraction. Data from Gill *et al.* (1964).

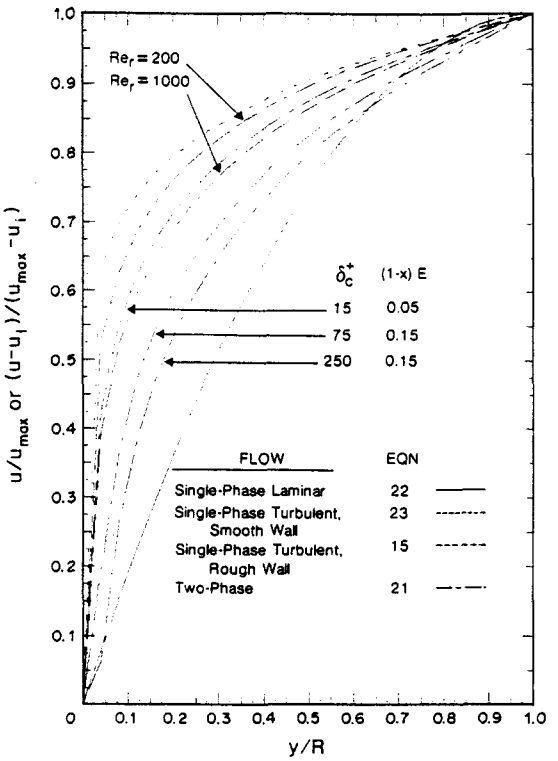

Figure 7. Comparison of predicted velocity profiles for different types of pipe flow.

addition to [14] for the single-phase turbulent flow with rough walls and [21] for the two-phase flow:

$$\text{laminar, } \frac{u}{u_{max}} = 1 - \left(\frac{y}{R}\right)^2; \qquad [22]$$

$$\text{turbulent, smooth wall } \frac{u}{u_{max}} = \left(\frac{y}{R}\right)^{1/7}. \qquad [23]$$

Typical values of the various parameters were used in the equations. The two-phase velocity profile clearly takes on a more laminar character with increasing $(1-x)E$. However, the two-phase flow is never purely laminar. While the presence of droplets does seem to suppress or dampen turbulent motion, even at small qualities or particulate loading there are significant changes in the velocity level and turbulence intensity (Theofanous & Sullivan 1982; Burdukov *et al.* 1979).

Gill *et al.* (1964), using the Von Karman velocity deficiency law for single-phase turbulent flow, calculated values of the Von Karman constant in the range of about $0.10 < k < 0.42$. The value generally decreased with increasing liquid flowrate above a flow of about 90 kg/h and with increasing air flowrate. With both liquid and vapor flows increasing there would be a tendency for more liquid to be entrained in the core of the annular flow. They suggested that increased entrained liquid would suppress turbulent eddies which would reduce the mixing length and, hence, the value of k. A second hypothesis was that the transition at about 90 kg/h in the k vs liquid flowrate curve occurs in the range in which large disturbance waves are formed and that these waves could affect the turbulence of the flow. However, entrainment will occur more readily with large waves than with small waves so the second hypothesis could be considered to be addressing the mechanism of the entrainment rather than a second mechanism for explaining the decrease in mixing length.

Data from high-pressure (68.6 b) steam flow follows the same pattern as the low-pressure air/water flow. The steam data are shown in figure 8. Insufficient information was given in the paper

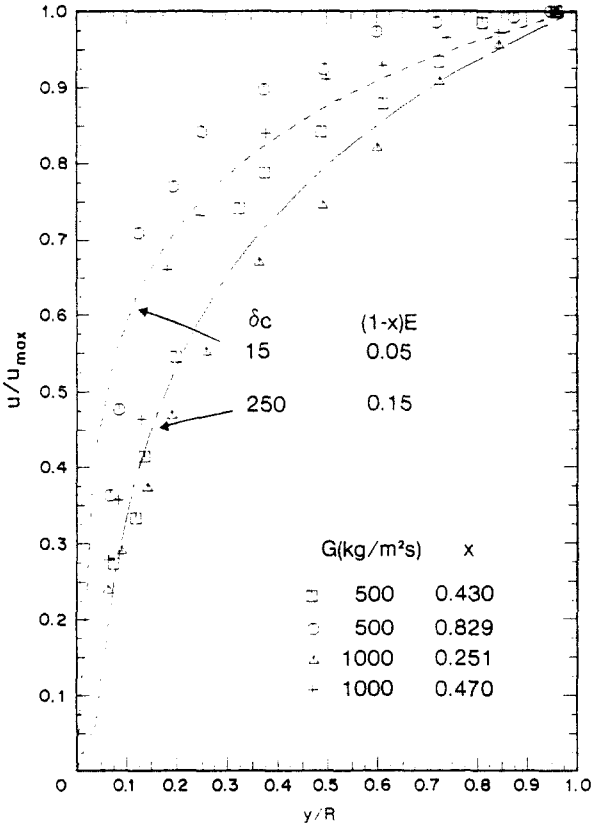

Figure 8. Qualitative comparison between high pressure steam/water velocity profiles and predicted velocity profiles. Data from Kashcheev & Muranov (1976).

by Kashcheev & Muranov (1976) to predict the velocity profiles with [21]. Thus, two predicted profiles with assumed parameters were plotted only for qualitative comparison purposes. As can be seen, as the quality increases for a given mass velocity the velocity profile becomes more blunt. This trend would be consistent with a decreasing entrained liquid fraction. Comparing the high-pressure steam data with the correlation developed with low-pressure air/water data shows that the general characteristics of the velocity profiles are the same for the two significantly different fluid conditions.

The data evaluated so far were from nonequilibrium flows but were taken far enough from the entrance ($L/D \simeq 167$) that the velocity behavior can be assumed to be only slowly changing. The velocity data from Gill *et al.* (1963a, b) were taken in the range $4.8 \leqslant L/D \leqslant 167$ for one liquid (454 kg/h) and one gas (227 kg/h) flow. Entrainment varied from 0.08 near the entrance to 0.53 near the exit. The data for this highly nonequilibrium experiment were also compared to the predictive equation with surprisingly good results. For 48 test runs with 619 data points the average ratio of predicted to experimental velocity was 1.09; the mean absolute deviation between the predictions and the data was 0.101; and the r.m.s. deviation was 0.150. As shown in figure 9 for the various test runs the predictions were high compared to the arithmetic average of the velocity profile data at each location near the inlet but decreased farther along the tube. It should be noted that the data from Gill *et al.* (1964) at the same fluid conditions as in Gill *et al.* (1963a, b) were also slightly overpredicted by 3–4%. Thus, it can be suggested that after $L/D > \sim 60$–70, there is very good agreement between the predictions and the data. This seems to indicate that the proposed velocity profile prediction method can handle nonequilibrium flows if the conditions are not changing too rapidly.

CONCLUSIONS

Several complete data sets from the literature were used to evaluate the triangular relationship between film thickness, film flowrate and pressure gradient. Three liquid film velocity profiles were

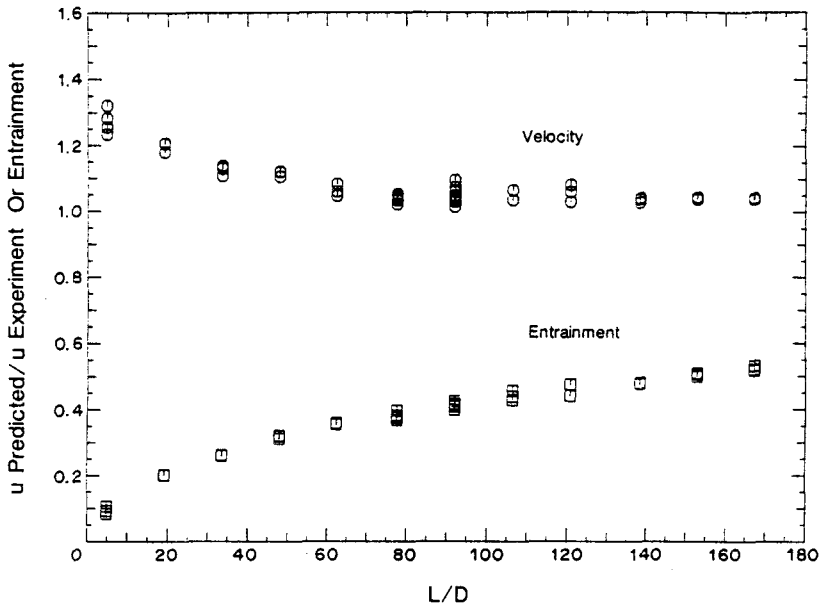

Figure 9. Comparison between predictive equation and highly nonequilibrium data. Data from Gill *et al.* (1964).

utilized in the evaluation. Comparison with data indicates that the double velocity profile method provides reasonably good predictions.

Experimental data from the core region of low-pressure air/water annular flow have been empirically correlated. The nondimensional velocity profile was found to be an explicit function of the nondimensional distance from the interface, total entrained liquid fraction and the liquid film thickness. It was concluded that the total entrained liquid fraction was responsible for the "laminarization" of the velocity profile. Quantitative agreement between the experimental air/water data and predictions from the correlating equation was good. Qualitative agreement between the equation and high-pressure steam/water flow indicated that the basic characteristics of the velocity profile are similar over large ranges of fluid conditions.

REFERENCES

ABOLFADL, M. & WALLIS, G. B. 1985 A mixing length model for annular two-phase flow. *PCH PhysicoChem. Hydrodynam.* **6,** 49–68.

ADORNI, N., CASAGRANDE, I., CRAVAROLO, L., HASSID, A. & SILVESTRI, M. 1960 Experimental data on two-phase adiabatic flow: liquid film thickness, phase and velocity distribution, pressure drops in vertical gas–liquid flow. Report CISE-R35.

ANDERSON, G. H. & MANTZOURANIS, B. G. 1960 Two-phase (gas–liquid) flow phenomena—I. Pressure drop and hold-up for two-phase flow in vertical tubes. *Chem. Engng Sci.* **12,** 109–126.

ANDREUSSI, P. & ZANELLI, S. 1979 Downward annular and annular-mist flow of air–water mixtures. In *Two-phase Momentum, Heat and Mass Transfer in Chemical, Process, and Energy Engineering Systems*, Vol. 1 (Edited by DURST, F., TSIKLAURI, G. V. & AFGAN, N. H.), pp. 303–314. Hemisphere, Washington, D.C.

BANKOFF, S. G. 1960 A variable density single-fluid model of two-phase flow with particular reference to steam–water flow. *J. Heat Transfer* **82,** 265–272.

BURDUKOV, A. P., KASHINSKY, O. N. & MUKHIN, V. A. 1979 Experimental investigation of turbulent transfer processes in gas–liquid flows. In *Two-phase Momentum, Heat and Mass Transfer in Chemical, Process and Energy Engineering Systems*, Vol. 2 (Edited by DURST, F., TSIKLAURI, G. V. & AFGAN, N. H.), pp. 959–971. Hemisphere, Washington, D.C.

CHIEN, S. F. & IBELE, W. 1964 Pressure drop and liquid film thickness of two-phase annular and annular-mist flows. *J. Heat Transfer* **86,** 89–96.

DOBRAN, F. 1983a Hydrodynamic and heat transfer analysis of two-phase annular flow with a new liquid film model of turbulence. *Int. J. Heat Mass Transfer* **26,** 1159–1171.

DOBRAN, F. 1983b Heat transfer in an upward flowing annular-dispersed flow. In *Interfacial Transport Phenomena HTD*-23 (Edited by CHEN, J. C. & BANKOFF, S. G.), pp. 93–99. ASME, New York.

DUKLER, A. E. & MAGIROS, P. 1961 Entrainment and pressure drop in cocurrent gas–liquid flow. Part II. Liquid property and momentum effects. *Dev. Mech.* **1,** 532–541.

GILL, L. E., HEWITT, G. F., HITCHON, J. W. & LACEY, P. M. C. 1963a Sampling probe studies of the gas core in annular two-phase flow—I. The effect of length on phase and velocity distribution. *Chem. Engng Sci.* **18,** 525–535.

GILL, L. E., HEWITT, G. F. & LACEY, P. M. C. 1963b Sampling probe studies of the gas core in annular two-phase flow. Part II. Studies of the effect of phase flow rates on phase and velocity distribution. Report AERE No. R.3955.

GILL, L. E., HEWITT, G. F. & LACEY, P. M. C. 1964 Sampling probe studies of the gas core in annular two-phase flow—II. Studies of the effect of phase flow rates on phase and velocity distribution. *Chem. Engng Sci.* **19,** 665–682.

HEWITT, G. F. & HALL-TAYLOR, N. S. 1970 *Annular Two-phase Flow*. Pergamon Press, Oxford.

ISHII, M. & ZUBER, N. 1979 Drag coefficient and relative velocity in bubbly, droplet or particulate flows. *AIChE Jl* **25,** 843–855.

KASHCHEEV, V. M. & MURANOV, Y. V. 1976 Calculation of velocity profile in two-phase disperse-annular flow. *High Temp.* **14,** 901–907.

KATAOKA, I. & ISHII, M. 1983 Entrainment and deposition rates of droplets in annular two-phase flow. In *Proceedings, ASME-JSME Thermal Engineering Joint Conference*, Vol. 1 (Edited by MORI, Y. & YANG, W. J.), pp. 69–80. ASME, New York.

KAYS, W. M. & CRAWFORD, M. E. 1980 *Convective Heat and Mass Transfer*, 2nd edn. McGraw-Hill, New York.

KUZNETSOV, Y. P. & DARMONO, R. 1978 Sand equivalent of phase interface roughness in descending two-phase annular flow. *Theor. Fdns chem. Engng* **12,** 318–324.

LEVY, S. 1966 Prediction of two-phase annular flow with liquid entrainment. *Int. J. Heat Mass Transfer* **9,** 171–188.

SCHENCK, H. 1979 *Theories of Engineering Experimentation*, 3rd edn. Hemisphere, Washington, D.C.

TATTERSON, D. F., DALLMAN, J. C. & HANRATTY, T. J. 1977 Drop sizes in annular gas–liquid flows. *AIChE Jl* **23,** 68–76.

THEOFANOUS, T. G. & SULLIVAN, J. 1982 Turbulence on two-phase dispersed flows. *J. Fluid Mech.* **116,** 343–362.

TURNER, J. M. 1966 *Annular Two-phase Flow*. Ph.D. Dissertation, Dartmouth College, N.H.

UEDA, T. & NOSE, S. 1974 Studies of liquid film flow in two-phase annular and annular-mist flow regions (Part II, upflow in a vertical tube). *Bull. JSME* **17,** 614–624.

UEDA, T. & TANAKA, T. 1974 Studies of liquid film flow in two-phase annular and annular-mist flow regions (Part I, downflow in a vertical tube). *Bull. JSME* **17,** 603–613.

VAN DER WELLE, R. 1981 Turbulence viscosity in vertical adiabatic gas–liquid flow. *Int. J. Multiphase Flow* **7,** 461–473.

WALLIS, G. B. 1969 *One-dimensional Two-phase Flow*. McGraw-Hill, New York.

WHALLEY, P. B., HEWITT G. F. & HUTCHINSON, P. 1974 Experimental wave and entrainment measurements in vertical annular two-phase flows. *Instn chem. Engrs Symp. Ser. No. 38, Multiphase Flow Syst.* **1,** 1–24.